INSTITUTE OF PHYSICS PUBLISHING JOURNAL OF PHYSICS B: ATOMIC, MOLECULAR AND OPTICAL PHYSICS

J. Phys. B: At. Mol. Opt. Phys. **34** (2001) L163–L172 www.iop.org/Journals/jb PII: S0953-4075(01)21092-X

LETTER TO THE EDITOR

The role of the potential saddle in He^{2+} + H impact ionization

Emil Y Sidky[1,3], **Clara Illescas**[2] **and C D Lin**[1]

[1] Department of Physics, Cardwell Hall, Kansas State University, Manhattan, KS 66506, USA
[2] Centre Lasers Intenses et Applications, Université de Bordeaux-I, F-33405 Talence, France

E-mail: sidky@phys.ksu.edu

Received 17 January 2001

Abstract
We compute the full three-dimensional momentum space distribution of ejected electrons resulting from alpha particle impact ionization of hydrogen. At low impact velocities the transverse momentum distributions are shown to exhibit strong oscillations with energy. For the longitudinal component, the momentum distribution peaks near the target at high energies, shifts towards the projectile centre at intermediate energies and then back towards the target at low energies. The shift of the longitudinal momentum distribution towards the target at low energies gives the experimental signature of the importance of potential saddle for impact ionization at low energies.

The saddle point mechanism (Winter and Lin 1984, Sidky *et al* 2000) for single ionization by ion impact has attracted much attention because of its potential to give a universal explanation for electron ejection in low energy ion–atom collisions. Briefly, the idea states that the active electron in an ion–atom collision can find itself balanced on the internuclear potential saddle during the collision. As the nuclei recede from each other the electron will remain at that point since the Coulomb forces from both nuclei balance at the saddle point, and the electron will be promoted up to the continuum as the saddle is pushed upward. Not only is this a simple explanation of an otherwise complicated three-body break-up process, but this mechanism can also explain single ionization of multi-electron atoms since the saddle point is far from the influence of any structure in either target or projectile ionic core. Moreover, this mechanism was thought to provide a unique signature in the distribution of ejected electrons; namely, the ejected electrons should move with the saddle velocity in the lab frame of reference. On the face of it the saddle point mechanism for ion impact ionization seems to be a well-defined, easily verifiable concept. But after its introduction in the early 80s, this mechanism has been the centre of much controversy (Stohlterfoht *et al* 1997).

Theoretically, it is clear that the saddle point promotion must occur, but the disagreement in the literature has centred on what range of impact velocities the saddle point mechanism

[3] To whom correspondence should be addressed.

is important. More critically, is it possible to make a semi-quantitative estimation for its importance? Olson and co-workers have been promoting the idea that the saddle point mechanism is most important for intermediate energy ion–atom collisions, where the total ionization cross section is the largest (Olson 1983, 1986, Olson *et al* 1987). Their identification of saddle point electrons was based on examining the longitudinal momentum distribution from classical calculations. They found that the distribution peaked at $v/2$, half the projectile velocity, coinciding with the potential saddle point velocity. It is not clear, however, that a $v/2$ peak uniquely identifies the saddle point mechanism, since the centre of charge and the saddle point coincide for singly charged ions impacting on neutral targets. Indeed, Sidky *et al* (2000) showed, using a combined quantum and classical analysis, that the saddle point mechanism is a low energy phenomenon and that the $v/2$ peak does not necessarily indicate that saddle point ionization is significant. This conclusion leads to the question of what happens in a system of asymmetric collisions such as α-particles impacting on a hydrogen atom, where the saddle point and centre of charge do not coincide.

Earlier classical work by Illescas *et al* (1998) explored the asymmetric α–H collision system. They concluded that the saddle point mechanism is important only at low impact energies. In this letter we explore the α–H system with both the quantum two-centre momentum space discretization (TCMSD) and classical trajectory Monte Carlo (CTMC) method, and we show quantitatively what the role of the saddle point mechanism is for ionization. Furthermore, we examine the longitudinal distribution and show that for this asymmetric system a shift, at low impact velocity, of the electron's longitudinal momentum distribution towards the saddle velocity *does* indicate saddle point ionization.

Another motivation for exploring ionization in α–H collisions stems from recent experimental results by cold target recoil ion momentum spectroscopy (Dörner *et al* 1996, Abdallah *et al* 1998a, b, 2000). Such experiments have measured the ejected electron momentum distribution (EEMD) for many ion–atom collision systems. An interesting feature that appears to be common to many ion–atom collision systems is the 'ubiquity of π structure' in the continuum (Abdallah *et al* 1998a). The asymmetry or symmetry of the transverse momentum distribution, however, varies greatly from system to system. For example, the transverse momentum distributions turned out to have strong energy dependence for some systems, e.g. p + He collisions, and little energy dependence for other systems, such as He^+ on He.

In this letter we explore ionization for an asymmetric, one-electron system, namely alpha particles on hydrogen. After a brief review of the TCMSD theory we will begin this letter by examining the EEMDs for α on H collisions and their energy dependence. We then outline the role of the saddle point mechanism for the α on H system, and finally derive a general scaling law for the range of saddle point ionization for arbitrary ion–atom collision systems. Our study of the He^{2+} + H system focuses primarily on impact velocity dependence of the transverse and longitudinal momentum distributions of the ejected electrons, and the dynamics of the ejected electron cloud are studied both quantum mechanically and classically. We select an impact parameter of two atomic units, since it is near the maximum of ionization probability and a previous CTMC study, with which we compare, concentrated on the impact parameter $b = 2$ au (Illescas *et al* 1998).

In the TCMSD theory, the electron wavefunction in the ion–atom collision is represented by a two-centre expansion in momentum space:

$$\begin{aligned}\Phi(\vec{p},t) &= \sum_{l,m} \tilde{T}_{l,m}(p,t)Y_{l,m}(\hat{p}) + \mathrm{e}^{-\mathrm{i}(\vec{p}\cdot\vec{R}-\frac{1}{2}v^2t)} \sum_{l,m} \tilde{P}_{l,m}(q,t)Y_{l,m}(\hat{q}), \\ \vec{q} &= \vec{p} - \vec{v}\end{aligned} \tag{1}$$

where the spherical harmonic $Y_{l,m}$ is defined with respect to each centre in the momentum space expansion and the phase factor in front of the second sum on the right is the plane-wave electron translation factor in momentum space. We have carried out a partial wave expansion on each centre and the radial functions, $\tilde{T}_{l,m}(p,t)$ and $\tilde{P}_{l,m}(q,t)$, are in turn expanded in B-splines. The details of the theory and the method of analysing the resulting wavefunction are described in previous references (Sidky and Lin 1998, 1999). The two-centre feature of the expansion in equation (1) allows an accurate representation of the electronic wavefunction with very few harmonics about each nuclear centre. In fact, including harmonics up to and including $l = 2$ on both centres was sufficient, just as was the case for the proton–hydrogen calculation (Sidky and Lin 1999).

In figure 1 we show the ejected electron momentum distribution for impact velocities $v = 0.5$, 0.6 and 0.7 au at $vt = 20$ au. We show the incoherent superposition of the ejected electron cloud from each nuclear centre, since doing so averages over the rapid time oscillation in the electron wavefunction (Sidky and Lin 1999). The distributions in the figure have been projected down onto the collision plane, and the curves shown on the right result from integrating over the longitudinal momentum in order to focus on the transverse momentum distribution. Interestingly, the behaviour of the α–H system at low velocity shows a rapid velocity dependence similar to what has been seen experimentally for the proton–helium and alpha–helium systems (Dörner *et al* 1996, Abdallah *et al* 1998a, b, 2000). The distribution is skewed to the opposite side of the projectile at $v = 0.5$ au, is almost symmetric at $v = 0.6$ au and finally goes towards the projectile at $v = 0.7$ au.

An interpretation of the rapid transverse oscillations at low impact velocities based on the molecular orbital concept has been addressed in terms of the hidden crossings theory of ion–atom collisions (Solov'ev 1989, Pieksma *et al* 1994). According to this model, one of the main mechanisms for ionization, called T-promotion, occurs through promotion of molecular states into the continuum as the target and projectile nuclei recede from each other. At small internuclear separations rotational coupling transfers population from σ orbitals to π orbitals and both types of orbitals are promoted to the continuum through T_{00} and T_{01} series of hidden crossings. The σ orbitals have no node across the internuclear line, while the π orbitals have one node transverse to the internuclear vector. The rapid velocity dependence is expected to come from the interference of σ and π amplitudes. But the hidden crossings theory cannot give the relative phase of the amplitudes. To obtain the phase information Macek and Ovchinnikov (1998) developed a two-state Sturmian model for the proton–hydrogen system where the relative phase between σ and π amplitudes has a rapid $1/v$ dependence. Thus, for p + H they predicted a strong velocity dependence for impact velocities below 1 au. In contrast, no such oscillations were predicted from our TCMSD and CTMC calculations for the p + H collisions (Sidky *et al* 2000).

The fact that we find a strong low velocity dependence on the transverse momentum distributions for the α–H system but not for the p + H system prompted us to investigate a possible interpretation in terms of σ–π interference. Within the framework of TCMSD we cannot uniquely determine a phase between σ and π amplitudes, since we do not expand the wavefunction in terms of molecular orbitals. Furthermore, there is an open question as to which translation factor to use for such orbitals. Using our two-centre expansion equation (1) in momentum space, we can easily inspect the atomic σ and π components on each centre where the axis of quantization is the collision axis. A prerequisite for interference is that σ and π amplitudes should be of the same order of magnitude. Since the relative phase is expected to vary as $1/v$, rapid oscillations in transverse momentum distributions at slow collision velocities are possible if the magnitudes of the σ and π components are comparable. In table 1, we compare the atomic probabilities on each centre for the α–H system at $vt = 20$ au. Clearly the σ and π amplitudes are of comparable magnitude for $v = 0.5$, 0.6 and 0.7 au

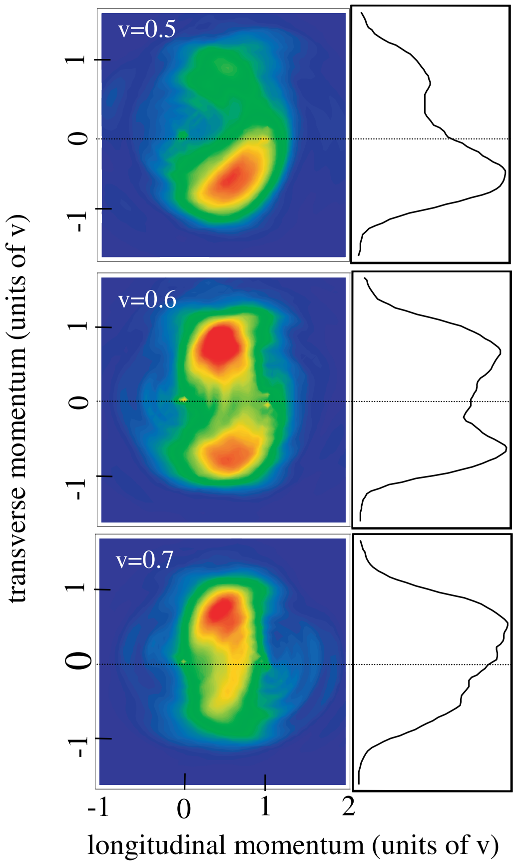

Figure 1. Quantum ejected electron momentum distributions, projected onto the collision plane, for α on hydrogen collisions at low impact velocity. Graphs on the right represent the projection of the total momentum distribution on to the transverse direction in the collision plane.

(This figure is in colour only in the electronic version, see `www.iop.org`)

making the interference to produce the rapid oscillations possible. Also, in table 1 we show the corresponding probabilities for p + H collisions at $vt = 20$ for $v = 0.45$, 0.63 and 0.78, or for collision energies of 5, 10 and 15 keV, respectively. For this system, the π component is much smaller than the σ component. Thus, σ–π interference plays little role in the velocity dependence of the EEMD, and we can understand quantitatively why rapid transverse momentum shifts do not occur in p + H collisions at low impact velocities.

According to the Sturmian model by Macek and Ovchinnikov, the σ–π phase is given by $1/v$ multiplied by an integral of the energy difference over the internuclear distance R. Thus we can expect oscillation in the transverse momentum to occur as a function of the internuclear separation R. In figure 2 we isolate the $v = 0.5$ au collision, and indeed from the TCMSD calculation (left column in the figure) oscillation does occur in the the transverse momentum as a function of vt. Note that at $vt = 5$ there is a very strong asymmetry in the transverse direction, which is a direct indication that the σ and π amplitudes are comparable in size and their relative phase is near zero. As vt increases, the transverse momentum distribution becomes symmetric (near $vt = 15$), corresponding to a relative phase near $\pi/2$. For increasing vt, the transverse momentum distribution then shifts to the other side as the phase increases towards π.

Table 1. Integrated probabilities of ionization into S ($l = 0$) and P ($l = 1$) harmonics on the target and projectile centres for α–H and p–H collisions. $P\sigma$ refers to the real $l = 1$ harmonic aligned along the collision axis and $P\pi$ refers to the real $l = 1$ harmonic aligned perpendicular to the collision axis and in the collision plane. All probabilities are multiplied by 10^3.

	Target			Projectile		
α–H	S	$P\sigma$	$P\pi$	S	$P\sigma$	$P\pi$
$v = 0.5$	7.51	5.67	4.67	3.18	3.98	1.30
$v = 0.6$	6.84	5.52	3.01	2.32	7.79	1.67
$v = 0.7$	13.93	5.37	5.44	1.67	12.83	7.01
p–H						
$v = 0.45$	31.64	1.85	1.22	37.17	1.24	3.49
$v = 0.63$	44.83	5.25	6.03	48.16	4.82	5.55
$v = 0.78$	55.87	7.20	5.93	50.15	6.36	6.22

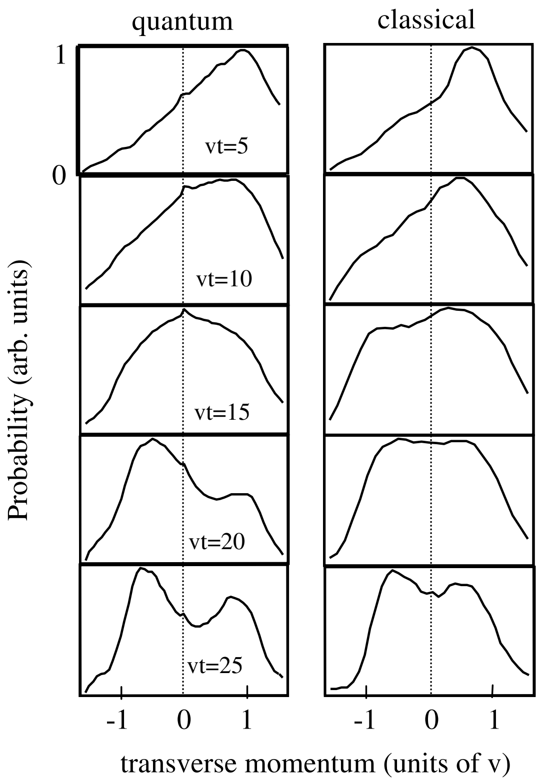

Figure 2. Evolution of the transverse momentum distribution of ejected electrons, resulting from an α–H collision at $v = 0.5$ au, as a function of internuclear separation after closest approach. The left column shows the quantum calculation, and the right column shows the classical calculation.

As in the previous study for p + H collisions (Sidky *et al* 2000) we have also carried out a CTMC calculation for the present collision system. In figure 2 we show the resulting transverse momentum distribution of ejected electrons. The classical distribution clearly shows the oscillation with respect to vt. However, the oscillation is shifted from the quantum result, going through a region where the distribution is nearly symmetric near $vt = 20$, and then swinging to the other side at $vt = 25$—see figure 2, right column. It is interesting to interpret the oscillation of the transverse momentum distributions classically. Recall that the potential in the transverse direction near the saddle is an attractive well. Classically, an electron under such a potential is expected to oscillate back and forth. This oscillation should occur for any collision system at low energies for each individual electron. The important feature of the CTMC calculation, shown in figure 2, is that the *ensemble* of ejected electrons oscillates, which follows from the fact that the transverse momentum distribution starts off highly asymmetric at $vt = 5$. A similar classical investigation of the p + H system at low impact velocity showed that the momentum distribution remains symmetric about $p_\perp = 0$ as a function of vt, while the individual electron trajectories oscillate (Sidky *et al* 2000).

One of the signatures of the saddle point ionization mechanism that experimentalists have been searching for is the so-called '$v/2$' peak in singly charged ion–atom collisions. Electrons promoted into the continuum by the potential saddle should have the same velocity as the saddle point—namely half the projectile velocity '$v/2$'. In a previous paper (Sidky *et al* 2000), however, we have shown that for protons on hydrogen collisions, the '$v/2$' peak does not provide sufficient evidence for claiming the existence of this ionization mechanism. It has been shown that for impact energies from 5 to 50 keV the longitudinal momentum distribution of ejected electrons peaks at $v/2$, while the saddle point mechanism is important only in the 5–15 keV region, accounting for about 1/3 of the total ionization according to the analysis of the classical calculations.

The α–H system allows us an opportunity to re-examine the correspondence between the saddle mechanism and a peak at the saddle velocity for a system where the saddle point is located at a different point to the centre of charge. In figure 3 the longitudinal momentum distributions of ejected electrons is plotted at low, intermediate and high impact velocities. At $R = 20$ both classical and quantum calculations are available, and they agree fairly well on the main features. At low impact velocity, $v = 0.5$, the classical calculation shows a well-focused peak at the saddle velocity. The quantum results also peak at the saddle velocity, but the distribution is markedly broader. (The difference in the 'sharpness' of the saddle peak between the classical and quantum calculations at low impact velocities comes from the fact that there is a sharp border in momentum between bound and continuum electrons classically, while no such well-defined border exists quantum mechanically). For the intermediate impact velocity, $v = 1.0$, the peak in the longitudinal momentum is slightly shifted towards the projectile at $R = 20$.

Looking to the CTMC curves corresponding to $vt = 500$ (the full curves in figure 3), the intermediate velocity collision changes dramatically with the longitudinal peak shifting towards the projectile velocity. The dramatic shift occurs at intermediate velocity, because the bulk of the ionization occurs shortly after the collision and the long-range Coulomb interaction pulls the continuum electrons closer to the higher charge. The low impact velocity collision shows a broader longitudinal distribution, stretched more towards the higher charge of the α-particle, but no significant shift in the *peak* position. The reason for this is that the saddle point mechanism is primarily responsible for ionization at $v = 0.5$, and there is no net force in the longitudinal direction that can pull the electrons away from the saddle point.

For the high velocity case in figure 3(*c*), $v = 3.0$, our calculations show the longitudinal peak to be near the target since soft electron emission is known to dominate for high energy collisions. To summarize, at high impact velocity we expect the longitudinal momentum distribution to peak near the target, and as the impact velocity is lowered towards the matching velocity ejected electrons longitudinal velocity should migrate towards the higher charged nucleus. Finally, as the impact energy is lowered even more the bulk of the ejected electrons should come away at the saddle velocity. For protons on hydrogen there is no shift between the

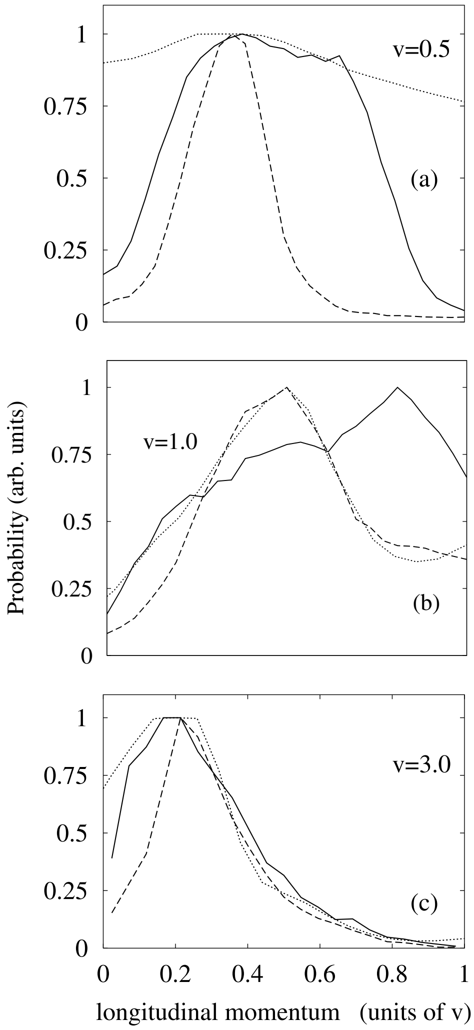

Figure 3. Comparison of quantum and classical longitudinal momentum distributions for all ejected electrons in an α on hydrogen collision at (*a*) $v = 0.5$, (*b*) $v = 1.0$ and (*c*) $v = 3.0$ au. The dotted curve is the quantum distribution at $vt = 20$; the dashed curve is the classical distribution at $vt = 20$ and the full curve is the classical distribution at $vt = 500$.

intermediate and low impact velocity case, since the centre of charge coincides with the saddle point. For He^{2+} colliding with hydrogen, the tell-tale shift of the longitudinal distribution going from intermediate to low impact velocities (the full curves in figures 3(*a*) and (*b*)) reveals the action of the saddle point mechanism.

Having revealed the effect of the saddle point mechanism in the final momentum distribution of ejected electrons in He^{2+}–H collisions, we now examine saddle point ionization as a function of internuclear distance during the collision. In our previous work (Sidky *et al* 2000) we found it useful to separate the ejected electrons into two categories as a function of internuclear distance: kinetic and saddle electrons. Kinetic electrons are those that have positive energy with respect to both nuclei, while saddle electrons are bound to one or other charge centre at the current R. The distinction between the two categories is physically motivated. The kinetic electrons exhibit primarily a free expansion from the collision centre while the saddle electrons have a more complicated trajectory due to the confining transverse potential. In Sidky *et al* (2000) the saddle electrons were mainly found to be within a minimum momentum

$$p_{\rm ion} = (2Zv/R)^{1/3}$$

of either nuclear centre (Z is the core charge of the respective nuclear centre). Since the minimum ionization momentum decreases with internuclear separation, the evolution of the ejected electron cloud separates into two distinct phases: first, at low R the circles of minimum ionization momentum overlap and the saddle velocity is less than $p_{\rm ion}$ away from both nuclear centres; second, as R increases, these circles shrink, eventually separating from each other. The transition between the two phases occurs at R^* which is the internuclear separation where the two circles touch and $p^T_{\rm ion} + p^P_{\rm ion} = v$. It is not difficult to calculate the formula for the transition radius

$$R^* = \frac{2}{v^2}(Z_T^{1/3} + Z_P^{1/3})^3. \tag{2}$$

R^* marks the internuclear separation where the saddle fraction decreases most rapidly. For internuclear separation less than the transition radius the saddle mechanism is still in play and the ejected electron distribution is still evolving, and for $R > R^*$ the basic shape of the EEMD is determined, though it may get distorted slightly by the long-range Coulomb forces.

Since R^* selects a common feature during the evolution of the EEMD of any ion–atom collision, it provides a natural scale for the internuclear separation. This scaling is demonstrated in figure 4, where the fraction of saddle electrons is plotted against the internuclear separation scaled to the transition radius. The curves shown result from low velocity collisions with α and proton projectiles impacting on hydrogen. Indeed the curves are all similar, differing only by a multiplicative factor on a log plot. The p+H collisions all show about the same saddle fraction, while the saddle fraction decreases with impact energy for He^{2+} + H. It is clear from figure 4 that saddle point ionization for He^{2+} + H is more important at low velocity than it is for p + H; we note that the total ionization cross section for the former collision system is lower by about a factor of two than the latter (Illescas and Riera 1999). Thus, we speculate that saddle point ionization has about the same effect in both systems, but prompt ionization is more difficult in the He^{2+} + H case since the electron must escape from a higher charge in the united atom limit. The scaling rule, equation (2), provides us with a simple way to know how far one must propagate the ejected electron distribution to establish its basic features. If one propagates the collision to three times R^*, for example, the saddle fraction is reduced to a negligibly small number. This is an extremely important law, since in practice it is not possible to extend numerical calculations to infinite internuclear separation, but with equation (2) one knows the minimum internuclear separation for establishing the structure of saddle point ionization.

In summary, we have applied the TCMSD method to finding the ejected electron distribution in alpha particle on hydrogen collisions. We find that the low energy behaviour of the ejected electron distributions are qualitatively different from the proton–hydrogen system; the former has a strong velocity dependence in the transverse momentum distributions and the latter a weak energy dependence. We have attributed this basic difference to the fact that the α–H system has comparable σ–π amplitudes in the continuum, while the p–H system has a much larger σ amplitude than π in the continuum. Interestingly, the classical calculations also show an oscillatory feature in the transverse momentum. As in the p + H system both the classical and quantum calculations agree on the general features of the ejected electron momentum distribution in α–H collisions. We have employed the classical calculation to see if the saddle point mechanism shows a distinguishing feature in the longitudinal momentum

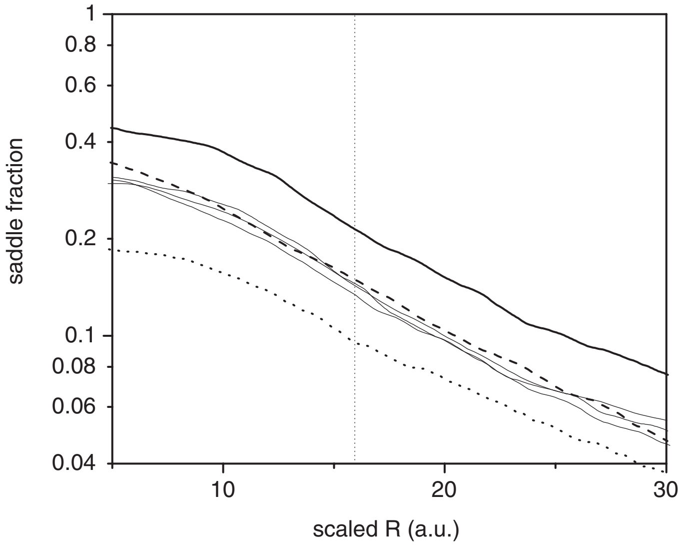

Figure 4. The ratio of the number of saddle electrons to all ejected electrons as a function of scaled internuclear separation. The thin full curves represent protons on hydrogen at impact energies 5 keV ($v = 0.45$ au), 10 keV ($v = 0.63$ au) and 15 keV ($v = 0.78$ au). (The same line type is used since these curves are nearly indistinguishable.) He^{2+} on hydrogen is shown for impact velocities 0.5 au (thick full curve), 0.7 au (dashed curve) and 1.0 au (dotted curve). The internuclear distance has been scaled by $16/R^*$, where 16 au is the critical internuclear separation, indicated in the figure by the vertical dotted line, for protons on hydrogen at $v = 1$ au. The ordinate is plotted on a logarithmic scale to illustrate that all the curves are the same apart from a multiplicative constant.

distribution at large internuclear separation. Indeed, for this asymmetric system we find that the momentum distribution peaks at the saddle for low velocity, and shifts *away* towards the higher charge at intermediate impact velocity when the saddle point mechanism is no longer important. Using the data from the p + H collision together with the α–H collision we have deduced a general scaling of the internuclear separation for ion–atom collisions which indicates when the saddle point mechanism can be considered to be over.

This work is supported by Chemical Sciences, Geosciences and Biosciences Division, Office of Basic Energy Sciences, Office of Science, US Department of Energy. CI would like to acknowledge support from the Ministerio de Educación y Cultura, Spain, for a Postdoctoral grant under the program SGPDE.

References

Abdallah M A, Cocke C L, Wolff W, Wolf H, Kravis S D, Stöckli M and Kamber E 1998a *Phys. Rev. Lett.* **81** 3627
Abdallah M A, Wolff W, Wolf H, Cocke C L and Stöckli M 1998b *Phys. Rev.* A **58** R3379
Abdallah M A, Wolff W, Wolf H, Coelho L F S, Cocke C L and Stöckli M 2000 *Phys. Rev.* A **62** 012711
Dörner R, Khemliche H, Prior M H, Cocke C L, Gary J A, Olson R E, Mergel V, Ullrich J and Schmidt-Böcking H 1996 *Phys. Rev. Lett.* **77** 4520–3
Illescas C, Rabadan I and Riera A 1998 *Phys. Rev.* A **57** 1809
Illescas C and Riera A 1999 *Phys. Rev.* A **60** 4546
Macek J H and Ovchinnikov S Y 1998 *Phys. Rev. Lett.* **80** 2298
Olson R E 1983 *Phys. Rev.* A **27** 1871
——1986 *Phys. Rev.* A **33** 4397
Olson R E, Gay T, Berry H G, Hale E B and Irby V D 1987 *Phys. Rev. Lett.* **59** 36

Pieksma M, Ovchinnikov S Y, van Eck J, Westerveld W B and Niehaus A 1994 *Phys. Rev. Lett.* **73** 46–9
Sidky E Y, Illescas C and Lin C D 2000 *Phys. Rev. Lett.* **85** 1634
Sidky E Y and Lin C D 1998 *J. Phys. B: At. Mol. Opt. Phys.* **31** 2949
——1999 *Phys. Rev.* A **60** 377
Solov'ev E A 1989 *Sov. Phys.–Usp.* **32** 228
Stolterfoht N, DuBois R D and Rivarola R D 1997 *Electron Emission in Heavy Ion-Atom Collisions* (Berlin: Springer)
Winter T G and Lin C D 1984 *Phys. Rev.* A **29** 3071